COLOR FILTERS: WHEN "OPTIMAL" IS NOT OPTIMAL

H. J. Trussell[1], *A. Ö. Ercan*[2], *N. G. Kingsbury*[3]

[1]Dept of Electrical and Computer Engineering, NC State University, Raleigh, NC
[2]Dept. of Electrical and Electronics Engineering, Özyeğin University, Istanbul, Turkey 34794
[3]Dept. of Engineering, University of Cambridge, Cambridge, CB2 1PZ, UK.

ABSTRACT

It is well known that many more than three or four spectral measurements are required for accurate measurement of color. Previous work has shown seven to ten measurements can yield accurate results on average, but with significant numbers of errors above the threshold of obvious visual detection. Furthermore, the filters used for these measurements are very difficult to fabricate. We show that such filters are not needed and, in fact, have much poorer performance, in perceptual quality measured in ΔE_{ab}, than simple narrow-band filters. This is especially true in the presence of Poisson noise at a level common in current digital cameras. In realistic Poisson noise, our filter sets of up to 12 filters allow average ΔE_{ab} values around 0.5, with maximum errors below 3.

Index Terms— Color image processing, spectral measurement

1. INTRODUCTION

It has been known for many years that in order to capture accurate color under varying illumination more than three or four color bands are required [1, 2, 3, 4, 5, 7, 6]. Commercial cameras are currently limited to this small number. Cameras used for archival recording are designed to work with a single illuminant in a controlled environment with many more filters [8, 9, 10, 11]. In this work, we consider optimal filters for cameras that can be used with varying illumination. Such filters could be used with a color mosaic that is larger than the current 2x2 arrays. Some work on larger arrays has begun. These extend the number of bands to five to seven bands and also address the necessary operation of demosaicking to obtain spectral estimates for each pixel [14, 6]. For example, a simulated 4×4 CFA pattern increases the number of measured spectral bands to 5 with a gain in color fidelity [6]. Unfortunately, this is not sufficient for the applications, such as textiles quality control [16], which require higher color accuracy.

Reducing the number of bands improves spatial resolution. The ultimate optimal trade-off in color accuracy versus spatial resolution remains a problem for the future that is likely to be determined by each manufacturer and relates to specific applications. The goal of this work is to lay a foundation by considering the criteria for selecting optimal filters for the fewest color bands required to obtain accurate color estimates in a realistic environment.

The capture of color information for a single reflectance sample by a P band sensor is modeled by

$$\mathbf{c} = \mathbf{S}^T \mathbf{L}_m \mathbf{r} + \eta, \tag{1}$$

where $\mathbf{r}$ is the $N \times 1$ reflectance vector, $\mathbf{L}_m$ is the $N \times N$ diagonal matrix representing the spectral power of the illuminant used for measurement, $\mathbf{S}$ is the $N \times P$ matrix representing the sensitivities of the P filter bands, η is the measurement noise, and $\mathbf{c}$ is the $P \times 1$ vector of measured values. The tristimulus values that define the color in CIEXYZ space are defined by

$$\mathbf{t} = \mathbf{A}^T \mathbf{L}_v \mathbf{r}, \tag{2}$$

where $\mathbf{A}^T$ is the $3 \times N$ matrix of CIE color matching functions, $\mathbf{L}_v$ is the $N \times N$ diagonal matrix representing the viewing illuminant, $\mathbf{t}$ is the 3×1 tristimulus vector.

It is clear that if the measuring illuminant is known and we can measure N independent bands of the spectrum, we can reconstruct the N-dimensional spectrum $\mathbf{r}$ and, thus, obtain perfect color measurement. Of course, a goal is to determine if a relatively small number of bands, $P << N$, will allow sufficient accuracy. The accuracy that is required is related to the perception of human observers. Thus, this accuracy will be measured by transforming the tristimulus values to CIELAB space and using the ΔE_{ab} color difference formulas [12].

The estimate of the reflectance uses the minimum mean square error (MSE) method that is given by:

$$\hat{\mathbf{r}} = \mathbf{\Sigma}_r \mathbf{S} [\mathbf{S}^T \mathbf{\Sigma}_r \mathbf{S} + \mathbf{\Sigma}_\eta]^{-1} (\mathbf{c} - \bar{\mathbf{c}}) + \bar{\mathbf{r}} \tag{3}$$

where $\mathbf{c}$ is the recorded values of the filter array, $\mathbf{\Sigma}_r$ is the covariance matrix of the reflectance ensemble, $\mathbf{\Sigma}_\eta$ is the covariance matrix of the noise, $\bar{\mathbf{c}}$ is the mean of the recorded values over the reflectance ensemble, $\bar{\mathbf{r}}$ is the mean of the reflectances.

2. FILTER DESIGN

The usual color filter design emphasizes creating filters that can include the space defined by the CIE color matching functions under various illuminants [15] or spans a subspace defined by the statisical characteristics of the reflectance data of interest [13]. The number of filters will vary depending on the accuracy of the final estimate of the spectrum that is desired. We will show that 12 or fewer simple Gaussian shaped filters will permit estimation with an average ΔE_{ab} error of less than 0.5 and maximum error of less than 3.0. These filter sets are easily approximated by current tunable methods [11].

Let us consider three ways of generating filters:

1. eigen filters: P non-negative filters created to span the P-dimensional space defined by the eigenvectors associated with the largest eigenvalues of the covariance matrix, $\mathbf{\Sigma}_{Tr}$, of the training set of interest. To make the filters less susceptible to noise, we choose the set of non-negative filters that is most orthogonal,by minimizing the condition number of the matrix containing the filters [13].

2. *ALm* filters: P non-negative filters created to span the P-dimensional space defined by the union of spaces defined by the color matching functions and the illuminants of interest, $\{\mathbf{L}_m\}_{m=1}^{M}$, $\mathbf{A}_M = [\mathbf{L}_1\mathbf{A}, \mathbf{L}_2\mathbf{A}, ..., \mathbf{L}_M\mathbf{A}^T]$. This set is a simple modification of that used by [2]. We again adjust to use the most nearly orthogonal set of non-negative filters that span the column space of $\mathbf{A}_M$. See Section 3.2 for more motivation.
3. Gauss filters: For the visual range of 380nm-730nm, we distribute the P filters uniformly and fix their standard deviation at half the distance between centers. This covers the range without leaving gaps. Experience has shown that this exact formulation is not critical.

3. NOISE ANALYSIS

3.1. Measurement Noise

For practical applications, we need to consider the effects of both measurement noise and quantization noise. Our work and others [13, 17] have indicated that the measurement noise, which is Poisson, dominates the quantization noise in current cameras. Since we are concerned with images captured by commonly available cameras that use 12 to 14 bits in the raw mode, we use 14 bit quantization for our simulations.

Previous work in choosing filters used 1% shot noise [13]. More recent work with common, high-end cameras gives a better model [16]. The relationship between the recorded pixel values, μ, and their variances, σ^2, was modeled by $\sigma^2 = \alpha\mu + \beta$, where the β is an offset applicable for measured data. Typical values for the model were $\alpha = 0.4$, and $\beta = -20$. The R^2 value for the fit for a Nikon D7000 was nearly 1.0. This was implemented in our simulations by scaling our filtered values to the range of those of the camera. We used a maximum camera value of 10000, rather than the absolute maximum of 16383 for 14-bit data to enable the range to agree with the data of [16]. Since the β offset is so small, we will omit it in the simulations. The recorded value of the filtered spectra in the camera domain is modeled as

$$t_k = \gamma c_k + \sqrt{\alpha\gamma c_k}\ \ \eta \tag{4}$$

where c_k is the ideal simulated output of the k^{th} filter,
$\gamma = max_{cam}/max_{sim}$ is the scaling factor used to adjust the range of the Poisson noise to the correct range, η is white Gaussian noise with zero mean and unit variance, and t_k is the recorded signal. We have used the scaled-Gaussian approximation to the Poisson distribution, since our light levels are assumed to be large.

For use in the MSE estimate, Eq.(3), the covariance, $\mathbf{\Sigma}_\eta$, which is related to the Poisson noise, is estimated using a diagonal matrix related to the variances of the noise in each filter measurement. The MSE estimate for the simulations is

$$\hat{\mathbf{r}} = \mathbf{\Sigma}_{Tr}\mathbf{S}[\mathbf{S}^T\mathbf{\Sigma}_{Tr}\mathbf{S} + \alpha \cdot diag(\mathbf{c})/\gamma]^{-1}(\mathbf{c} - \bar{\mathbf{c}}) + \bar{\mathbf{r}} \tag{5}$$

where $\mathbf{c}$ comprises the recorded values from the filter array, $\mathbf{\Sigma}_{Tr}$ is the covariance matrix of the training dataset (estimator of $\mathbf{\Sigma}_r$), $\bar{\mathbf{c}}$ is the mean of the recorded values over the training set, $\bar{\mathbf{r}}$ is the mean of the reflectances over the training set, and the constants α and γ are defined by Eq.(4).

3.2. Metamerism Noise

We now introduce a different type of noise that is related to relationships between the space defined by the measurement filters and the space defined by the CIE color matching functions and the viewing illuminant. From [15], we know the reflectance can be decomposed into the portion in the visual space (span of row vectors of $\mathbf{A}^T\mathbf{L}_v$, denoted $span(\mathbf{A}^T\mathbf{L}_v)$ hereafter) and its complement, known as the black space. The tristimulus values depend only on the projection of $\mathbf{r}$ onto the visual space. Call this projection operator, $\mathbf{P}_v$, and its complementary projection onto the black space, $\mathbf{P}_b = \mathbf{I} - \mathbf{P}_v$. Thus, we have

$$\mathbf{t} = \mathbf{A}_v^T\mathbf{r} = \mathbf{A}_v^T\mathbf{P}_v\mathbf{r}, \tag{6}$$

where $\mathbf{A}_v^T = \mathbf{A}^T\mathbf{L}_v$.

The span of the measurement filters with the measurement illuminant, $span(\mathbf{S}_m^T)$, where $\mathbf{S}_m^T = \mathbf{S}^T\mathbf{L}_m$, may not match that of the visual space under the viewing illuminant, i.e., $span(\mathbf{A}_v^T)$. In order to capture all of the information needed to determine the tristimulus values under the viewing illuminants of interest, the $span(\mathbf{S}_m^T)$ must contain the span of $\mathbf{A}_k^T$ for all k illuminants.

Consider the projection of $\mathbf{r}$ onto the measurement space, defined by the operator, $\mathbf{P}_m = \mathbf{S}_m(\mathbf{S}_m^T\mathbf{S}_m)^{-1}\mathbf{S}_m^T$. Similarly, let $\mathbf{P}_v$ define the projection onto the viewing space, the $span(\mathbf{A}^T\mathbf{L}_v)$. Using linear methods, the best we can do from the measurements is to recover the part of the reflectance that is projected onto the viewing space. The spectral error is $\mathbf{e} = \mathbf{P}_v\mathbf{r} - \mathbf{P}_v\mathbf{P}_m\mathbf{r} = \mathbf{P}_v\mathbf{P}_{bm}\mathbf{r}$, where $\mathbf{P}_{bm} = \mathbf{I} - \mathbf{P}_m$.

For a given viewing illuminant, we write $\mathbf{r} = \mathbf{P}_v\mathbf{r} + \mathbf{P}_b\mathbf{r}$. Any nonzero $\mathbf{P}_b\mathbf{r}$ defines a metamer of $\mathbf{P}_v\mathbf{r}$, since $\mathbf{A}^T\mathbf{L}_v\mathbf{P}_b\mathbf{r} = \mathbf{0}$. The error depends only on the part of $\mathbf{r}$ that is in the black space of the measurement space, in other words, the part of $\mathbf{r}$ that is in the viewing space but not captured by the sensors. This missing part of the spectrum of $\mathbf{r}$ is what we will refer to as metamerism noise.

3.3. Relation of measurement and metamerism noise

The noisy, measured values are given in Eq.(1), where η is the Poisson measurement noise. The error in the tristimulus values is $\mathbf{e} = \mathbf{A}_v^T(\mathbf{P}_v\mathbf{r} - \mathbf{P}_v\mathbf{P}_m\mathbf{r})$. By substitutions, this can be written as

$$\mathbf{e} = \mathbf{A}_v^T\mathbf{P}_{bm}\mathbf{r} - \mathbf{A}_v^T\mathbf{S}_m(\mathbf{S}_m^T\mathbf{S}_m)^{-1}\eta \tag{7}$$

where the first term is the metamerism error and the second term is the error caused by measurement noise.

To get an idea of the relationship between the measurement and metamerism noises for a given filter set, we compute the error variances of the two terms of Eq.(7). Since this error is in the tristimulus domain, the signal is the correct tristimulus values, i.e., $\mathbf{A}_v^T\mathbf{r}$, for each measurement/viewing illuminant. For this experiment, the viewing and measurement illuminants are the same. Figure 1 summarizes the two types of error for four different illuminants D65 (daylight)[12], A (incandescent)[12], F2 (cool white fluorescent)[12] and LED (white indoor lighting)[22], shown in Fig. 5, and the three filter sets. The illuminants are normalized to a maximum value of 100. The errors for the Munsell sample training set [18] are shown as Signal-to-Noise Ratio (dB), so higher is better.

$$SNR_{dB} = 10\log_{10}\left(\frac{\sum_{k=1}^{K}||\mathbf{t}_k||^2}{\sum_{k=1}^{K}||\mathbf{e}_k||^2}\right), \tag{8}$$

where $\mathbf{e}$ is one of the two error types of Eq.(7).

We can see that the error is dominated by the measurement noise for almost all filters. The metamerism SNR improves with the number of filters, as does the error caused by the Poisson noise. The metamerism SNR is usually better for the filters derived from the optimal eigenvectors, especially the ALm filter results. However, the SNR from the Poisson noise is always better for the Gaussian filters. This result is seen in the figure bars for measurement noise.

3.4. Figure of Merit Analysis

The figure of merit (FOM) of [21] can be used to predict the performance of a filter set in the presence of noise. This measure includes the effects of the distribution of the reflectance samples and the perceptual space in which we are interested. The FOM has a range of [0,1] with unity representing perfect color reproduction. In Figures 2 and 3, we give the figures of merit of the "optimal" eigenvector-based set, the ALm set and the uniformly spaced Gaussian set in both the noiseless and noisy cases, respectively. From Figure 2, we see that the ALm filters are always rated better in the noiseless case. The Gaussian filters perform surprisingly well and are superior to the eigen filters for higher numbers of filters. From Figure 3, we see that the Gaussian filters are always rated better in the noisy case, except for the D65 illuminant for 8 filters. In Figure 4, we show the Noise susceptability, which is defined as the difference between the Noiseless FOM and the Noisy FOM. The Gaussian set is clearly less susceptible to noise than either the eigen or ALm sets.

Key for Figures: FNXXX indicates using N filters under illuminant XXX, e.g., F10D65 indicates 10 filters under D65, F8F2 indicates 8 filters under F2 illuminant.

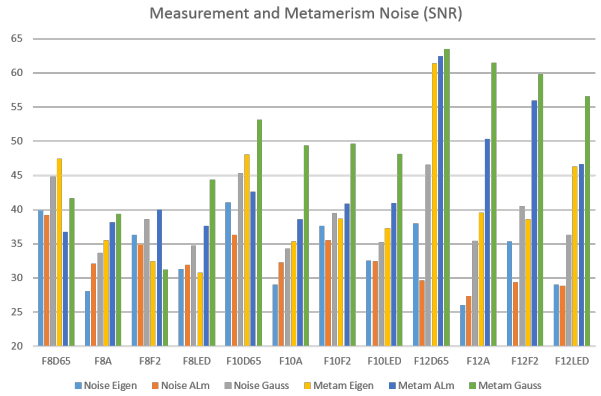

Fig. 1. Measurement and Metamerism Signal/Noise Ratios

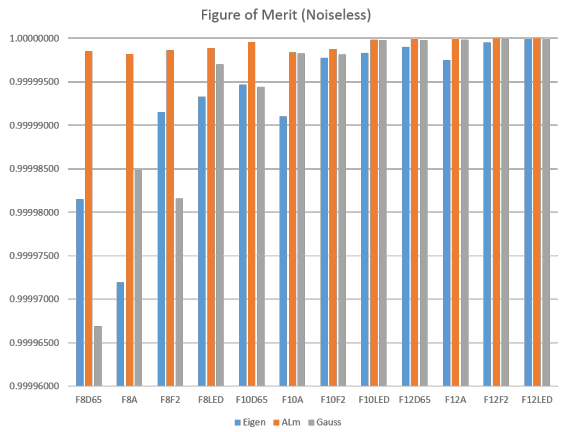

Fig. 2. Figure of Merit: Noiseless

4. RESULTS

We now test the performance of the filter sets on a standard spectral dataset, the Munsell set of 1269 samples [18]. The filters are required to work in a camera, so we must use different illuminants to simulate different viewing conditions. Most current cameras have adjustments for the viewing illuminant. Thus, we will assume for this work that the measuring illuminant and the viewing illuminant are identical i.e., $\mathbf{L}_m = \mathbf{L}_v$. The problem of estimating the color under mismatched illuminants is left for later work. We use the illuminants of Fig. 5.

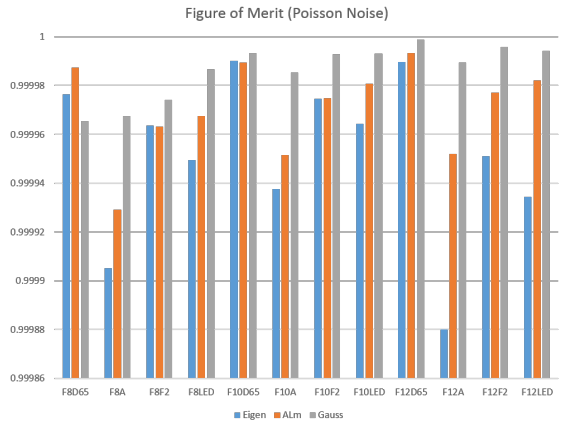

Fig. 3. Figure of Merit: Poisson Noise

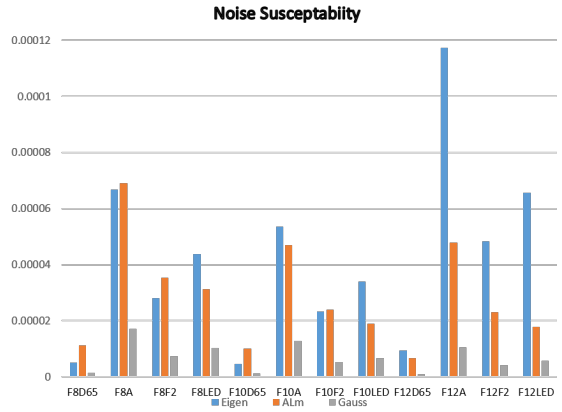

Fig. 4. Figure of Merit: Noise Susceptability

We obtain the simulated measured data, Eq.(7), for each of the filter sets, for each illuminant and for both the noiseless case and the simulated Poisson noise. The estimation of the spectra and the resulting CIELAB values use the MSE method of Eq.(5).

We used a training set of 300 random examples from the Munsell reflectance database [18] for "optimal" filter design. We tested the performance of the filters using a different set of 300 samples from the same ensemble. This was repeated for five different random samplings of the Munsell ensemble. For the noisy simulations, we added five realizations of noise for each sample set (25 simulations). Similar results were obtained training and testing using a textiles database [19].

We show both the average ΔE_{ab} error and the maximum error of the test sets, i.e., the average over the five samples and the maximum over the five samplings. The maximum error is particularly important since it indicates the worst case. For evaluation in the textiles industry, an error of greater than 1.0 usually means the difference between acceptance and rejection.

The results shown in Fig. 6 demonstrates the ALm set performs very well in the noiseless case, as expected from the analysis of metamerism noise and the FOM. However, the Gaussian filter does about as well for 10 and 12 filters. In the noisy cases shown in Fig. 7, the Gaussian filter sets substantially outperform the other two sets.

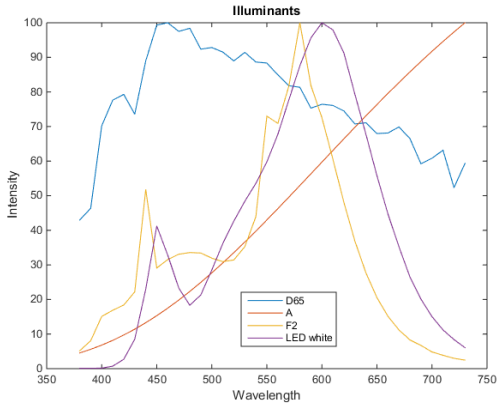

Fig. 5. Illuminants used for simulations

This is very good news, since those filters are much easier to fabricate than the "optimal" filters. Note that we have truncated the perceptual errors in the graphs to better show the combination of values for noiseless and noisy. Perceptual values above 10 are obviously easily perceived and the relative values above this are not important.

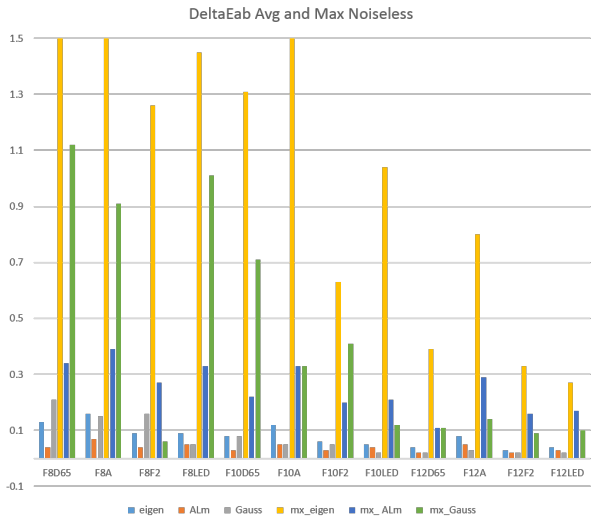

Fig. 6. ΔE_{ab} errors: average and max, noiseless data

Since the estimation is based on minimizing the MSE of the spectral error, it is reasonable to show those errors and relate them to the perceptual errors of Figures 6 and 7. The spectral errors for these cases are shown in Figure 8. We truncate the spectral errors to better show the smaller values. It is noted that increasing the number of filters also results in lowering the MSE of the spectra for all cases. However, we see that a smaller spectral error does not always produce a smaller perceptual error. This is not surprising, since the ALm sets were designed to cover the CIE color spaces, while the eigen set was designed to reproduce the entire spectrum, which may have a significant part in the black space.

We also tested to check the sensitivity of the method to specific qualities of a particular ensemble. We varied the combinations of training and test sets. We experimented with databases of textile samples [19], Dupont Automotive paint samples [20] along with the Munsell set in variations as training and test sets. We summarize these results as: for fewer filters and the eigen and ALm filter sets the effect of the mismatch is significant. For the Gaussian filters and

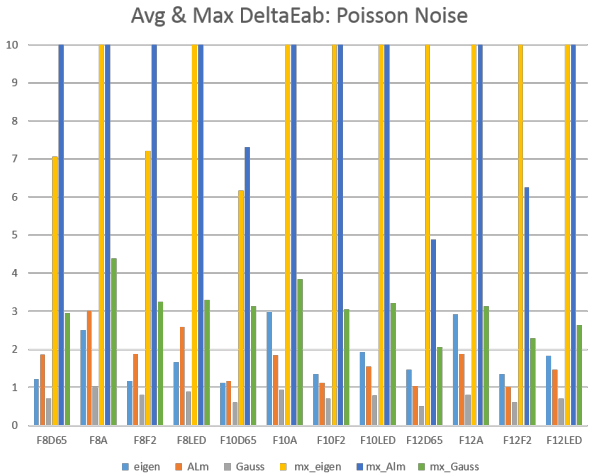

Fig. 7. ΔE_{ab} errors: average and max, noisy data

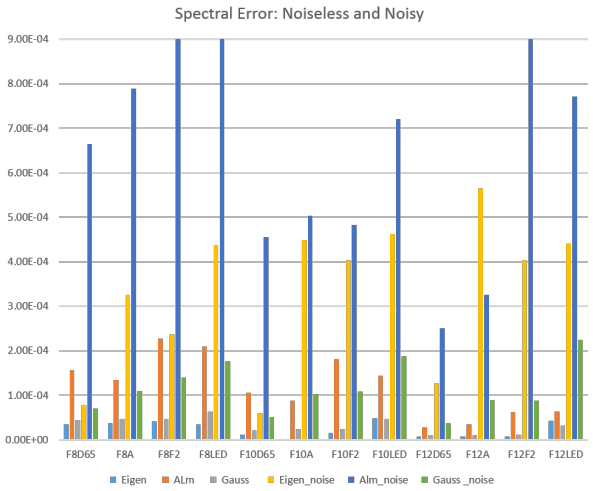

Fig. 8. Average Spectral Errors: noiseless and noisy data

larger number of filters, the effect is quite small, since that filter set does not depend on a training set.

5. CONCLUSIONS

We have shown that color filters designed to capture accurate color in the presence of the dominant Poisson noise should not follow the usual rules for optimization. The filters that are, in theory, best matched to the data or color spaces are not optimal in the presence of the actual noise encountered in common digital cameras. While this work has not determined the most optimal filters, it has indicated that the cheaper and more realizable narrowband filters are very good.

Preliminary investigations have shown that variations of the width of the Gaussian filters does not improve performance above that of the sets presented here. We have not investigated a change in the spacing or distribution of the filters.

Our work has also indicated that there may be a limit on the accuracy of high-resolution cameras with the current level of Poisson noise. The noise may be reduced by averaging over a small region of the same color. This represents a further trade-off between color accuracy and spatial resolution.

6. REFERENCES

[1] M. J. Vrhel and H. J. Trussell, "Filter Considerations in Color Correction," IEEE Trans. Image Processing, Vol. 3, No. 2, pp. 147-161, March 1994.

[2] M. J. Vrhel and H. J. Trussell, "Optimal Color Filters in the Presence of Noise," IEEE Trans. Image Processing, Vol. 4, No. 3, June 1995.

[3] M. Wolski, C. A. Bouman, J. P. Allebach, E. Walowit, "Optimization of Sensor Response Functions for Colorimetry of Reflective and Emissive Objects," IEEE Trans. Image Proc., Vol. 5, NO. 3, pp. 507-517, Mar. 1996

[4] H. Kuniba, R. S. Berns, "Spectral sensitivity optimization of color image sensors considering photon shot noise," Journal of Electronic Imaging Vol. 18, No. 2, 023002, Apr.–Jun. 2009

[5] M. Parmar, S. J. Reeves, "Selection of optimal spectral sensitivity functions for color filter arrays," IEEE Trans. Image Proc., Vol. 19, NO. 12, pp. 3190-3203, Dec. 2010

[6] Y. Monno, S. Kikuchi, M. Tanaka and M. Okutomi, "A practical one-shot multispectral imaging system using a single image sensor," *IEEE Trans. Image Processing,* Vol. 24, No. 10, pp. 3048-3059, 2015.

[7] N. Shimano, "Optimization of spectral sensitivities with Gaussian distribution functions for a color image acquisition device in the presence of noise," Optical Engineering, Vol. 45, No. 1, January 2006

[8] H. Maitre, "15 years of image processing and the fine arts," Proc. IEEE Int. Conf. on Image Proc., 557 - 561 vol.1, Oct. 2001, Thessaloniki, Greece.

[9] M. Barni, A. Pelagotti, A. Piva, "Image Processing for the Analysis and Conservation of Paintings: Opportunities and Challenges," IEEE Signal Processing Magazine, Vol. 22, No. 5, pp. 141-144, Sept. 2005

[10] A. Pelagotti, A. Del Mastio, A. De Rosa, A. Piva, "Multispectral imaging of paintings," IEEE Signal Processing Magazine, Vol. 25 , No.4, pp. 27 - 366, July 2008

[11] R. S. Berns, B. D. Cox, F. M. Abed, "Wavelength-dependent spatial correction and spectral calibration of a liquid crystal tunable filter imaging system," Applied Optics, Vol. 54, No. 12, pp. 3687-3693, April 20, 2015

[12] CIE. Colorimetry. Vienna: CIE Publication No. 15.2, Central Bureau of the CIE; 1986.

[13] D.Connah, A. Alsam, J. Y. Hardeberg, "Multispectral Imaging: How Many Sensors Do We Need?" J. of Imaging Science and Technology, Vol. 50, No. 1, pp.45-52, 2006.

[14] F. Yasuma, T. Mitsunaga, D. Iso, S. K. Nayar "Generalized Assorted Pixel Camera: Postcapture Control of Resolution, Dynamic Range, and Spectrum," IEEE Trans. Image Proc., Vol. 19, NO. 9, pp. 2241-2253, Sept. 2010

[15] H. J. Trussell and M. J. Vrhel, *Fundamental of Digital Imaging*,Cambridge University Press, 2008.

[16] R. Cao, "Development of Instrumental Techniques for Color Quality Control of Complex Colored Pattern," Dissertation, NCSU 2015

[17] H.J. Trussell, R. Zhang, "The Dominance of Poisson Noise in Digital Cameras," IEEE Int. Conf. Image Proc., 30 Sept.-3 Oct. 2012, Orlando, FL

[18] http://cs.joensuu.fi/s̃pectral/databases/download/munsell_spec_matt.htm

[19] A. Shams-Nateri, "Measuring Reflectance Spectra of Textile Fabrics by Scanner," J. Textile Science and Engineering, Vol. 102, pp. 1-13, 2011.

[20] M. J. Vrhel, R. Gershon, and L. S. Iwan, "Measurement and Analysis of Object Reflectance Spectra," Color Research and Application, vol. 19, pp. 4-9, 1994.

[21] G. Sharma and H. J. Trussell, "Figures of Merit for Color Scanning Filters," IEEE Trans. IP, Vol. 6, No. 7, pp. 990-1001, July 1997.

[22] H. Mirzaei and B. Funt, "Metamer Mismatching as a Measure of the Color Rendering of Lights," Proc. AIC 2015 International Colour Association Conference, Tokyo May 2015.